

Eco-friendly synthesis of *Syzygium aromaticum* titanium dioxide nanoparticles (SATiO₂NPs), characterization, and their application

Anju Meena¹, Dr. Pallavi Sharma²

¹Research Scholar, Maa Bharti PG College, University of Kota, Kota, (Rajasthan) India ²Associate Professor, University of Kota, Kota, (Rajasthan), India

ABSTRACT

A reliable and environmentally friendly method for synthesizing Titanium dioxide (TiO₂) nanoparticles has been developed using plant extracts. Characterization was carried out through UV-visible spectroscopy, Fourier Transform Infrared Spectroscopy (FTIR), and X-ray diffraction (XRD). This approach offers a simple and effective way to produce TiO₂ nanoparticles for dye reduction applications. The buds of *Syzygium aromaticum* served as a capping or reducing agent. The UV-visible spectra showed peaks between 350 and 400 nm, confirming the successful synthesis of nanoparticles. A Zeta Sizer measured the average particle size at 329.5 nm, indicating some aggregation of smaller particles. XRD patterns exhibited characteristic Bragg peaks consistent with the anatase phase, which has a tetragonal crystal structure. The *Syzygium aromaticum*-derived TiO₂ nanoparticles showed a significant decrease in dye absorbance: 90.5% at 554 nm for Rhodamine B, 81.68% at 564 nm for Bromophenol Red, and 71.41% at 557 nm for Phenol Red. The potential use of these nanoparticles in dye degradation was completed within 20 minutes. Green synthesis of nanoparticles holds promise for applications across various fields, including wastewater treatment, antibacterial, and antifungal activities.

Keywords- SATiO2NPs, UV-visible spectra, XRD, FTIR, Rhodamine B, Bromophenol Red, Phenol Red.

INTRODUCTION

Nanotechnology is one of the modern techniques. Small-sized nanoparticles exhibit enhanced or different properties compared to the bulk material. The tiny size of nanoparticles provides a large surface area relative to their volume and serves as a stabilizing agent in nanoparticle synthesis methods. The most studied nanoparticles today are those made from noble metals, particularly silver (Ag), platinum (Pt), gold (Au), titanium dioxide (TiO₂), and palladium (Pd). Environmental toxicity is a major concern in physical and chemical synthesis methods. Therefore, there is an emerging need for alternative sources for nanoparticle synthesis (Nayantara et al.,2018). Green synthesis of nanoparticles via extracts from bacteria, mushrooms, yeast, and plant parts presents an ideal alternative for environmentally friendly nanoparticle synthesis. Due to their small size and large surface area, nanoparticles possess unique catalytic, optical, magnetic, and electrical properties. Environmentally friendly synthetic TiO₂ nanoparticles can be utilised as plant nutrient fertilisers to enhance plant production. Nanoparticles are increasingly found in the fields of medicine, electronics, sensors, optical systems, catalysts, photographic electrochemical devices, medicinal products, biosensors, organic imaging, antibacterial applications, food preservation, and photonics (Raliya, R., et al., 2015).

Syzygium aromaticum belongs to the Myrtaceae family and is frequently used as a preservative due to its effective antibacterial properties. The flower buds contain the highest concentration of essential oils within the plant. Cloves have garnered significant attention for their antioxidant, antinociceptive, antibacterial, antiviral, and cytotoxic properties. This plant is one of the most important sources of phenolic compounds, including flavonoids, hydroxycinnamic acids, hydroxybenzoic acids, and hydroxyphenyl propenes. Clove is particularly valued for its phenolic compounds, such as quercetin and kaempferol, which possess antioxidant, anti-inflammatory, and anticancer properties; ellagic acid, a hydrolyzable tannin known for its anticancer and antioxidant effects; and caffeic and ferulic acids, which are often used in skincare products. Eugenol, the main compound found in clove, is utilized in flavouring, aromatherapy, topical medications, cosmetics, and perfumery. It has been employed in dental applications for its pain relief and anti-inflammatory properties (Maggini et al., 2024; Hameed et al., 2021; Lakhan et al., 2020; Ricardo-Rodrigues et al., 2024; Singh et al., 2024; Edis Z., 2025).



Currently, green synthetic strategies using plant extracts have been actively applied to produce TiO₂NPs: *Phyllanthus niruri* leaf extract (Panneerselvam, A., et al., 2020), *Syzygium cumini* leaves extract (Khan, A., et al., 2024), *(Garcinia mangostana*) Pericarp Extract (Ahn, E. Y., et al., 2022), *Azadirachta indica* (Krishnasamy, A., et al., 2015), *Solanum Tuberosum* (Girigoswami et al., 2024), *Solanum Tuberosum* (Girigoswamia, A., et al., 2024) *Aloe barbadensis* [Rajkumari J., et al., 2019], *Citrus limon* [Hossain A., et al., 2019], *Trigonella foenum-graecum* [Subhapriya S., et al., 2018], *Cochlospermum gossypium* [Saranya, K.S., et al., 2018], *Jatropha curcas L* (Goutam, S.P., et al., 2018) and *Eichhornia crassipes* [Zhang Y., et al., 2023].

Titanium dioxide is a widely recognized and thoroughly researched material due to its stable chemical structure and impressive physical, optical, and electrical properties, including biocompatibility [Bryanvanda, M. M., 2013]. Titanium dioxide has garnered significant attention from scientists for its potential applications in advancing technology within electronics, materials science, and medicine at the nanoscale. Thanks to its optical features, exceptional chemical stability, and non-toxic nature, titanium dioxide (TiO₂) serves as an eco-friendly photocatalyst. TiO₂ is characterized as a white pigment and a strong, lustrous, and degradable metal. Its applications extend to the production of colorants, plastics, paper, ink, rubber, textiles, automotive materials, cosmetics, leather, air purification products, industrial photocatalysis, organic matter decomposition, and ceramics, among others. TiO₂ is a major semiconductor in dyesensitized solar cells (DSSCs) (Hsu, C., Mahmoud, et al., 2024). Its photocatalytic characteristics are utilized for purifying air and water by removing contaminants [Bryanvanda, M. M., 2013].

Water pollution stands as a pressing concern today. Industries such as textile and paper frequently discharge large quantities of synthetic organic dyes into water bodies without adequate treatment. The release of these toxic dyes negatively impacts water quality, leading to severe potential health risks, including cancer and other ailments in aquatic life, animals, and humans. Approximately 7–10 percent of the textile industry contributes to the release of 5 tons of dye materials into the environment. Currently, there are about 10,000 different dye colors available for commercial use. Data shows that most of these dyes are highly toxic and carcinogenic, posing significant risks of kidney issues, liver damage, and cancer. Various techniques, such as flocculation, electrocoagulation, UV-light degradation, and activated carbon, have been employed to degrade toxic organic dyes. Although adsorption, ion exchange, and flocculation have been previously used to alleviate the harmful effects of these dyes, they have not effectively eliminated or degraded the substances completely, thus contributing to ongoing environmental pollution. Among the various dye removal methods, the bionanotechnology-based degradation approach is viewed as the most efficient way to eliminate dye pollutant residues. Consequently, there is an urgent need to adopt novel strategies to mitigate the harmful effects of textile dyes through degradation using nanocatalysts synthesized via a green chemistry approach (Sowmya M. et al., 2023). Various types of color dyes are generally used in the textile industry for coloring fabric production. And utilized by 10-15% for producing colored fabrics in the textile industry. About 7-105 tons of dye substances are being released into the environment from textile industries alone. Almost 10,000 different colors of dyes are presently available for commercial applications. It is reported that most color dyes are highly toxic and carcinogenic to humans and animals and are also responsible for causing kidney problems, liver damage, and cancer (Aswini, R., 2021).

This work presents a novel green synthesis approach for the preparation of titanium dioxide nanoparticles using *Syzygium aromaticum* extract as a reducing agent. The nanoparticles were studied for catalytic dye degradation.

MATERIAL AND METHODS

Titanium dioxide (no purification is needed) of analytical grade was purchased from RANKEM Laboratory Reagent (Avantor), ethanol, sterile distilled water, Whatman filter paper No. 1, NaBH₄ purchased from LOBA CHEMIE PVT LTD, and all the other chemicals used in the proposed study were of analytical grade. Rhodamine B (RhB) ($C_{28}H_{31}ClN_2O_3$, MW 479.01 g/mol), Phenol red (PR) ($C_{19}H_{14}O_5S$ and MW 354.38 g/mol), and Bromophenol red (BPR) ($C_{19}H12Br_2O_5S$ and MW 512.17 g/mol) were purchased from Sigma-Aldrich and used without further purification. These dye stock solutions were prepared by dissolving a suitable amount of dye powder in distilled water. NaBH₄ solution should always be prepared fresh.

Preparation of Syzygium aromaticum buds' extract:

Buds of *Syzygium aromaticum* were carefully collected from the market. Healthy, elongated buds were rinsed multiple times with distilled water to remove dust particles. The buds were dried in an oven at 40 °C until fully dry. A powder was prepared from the dried buds using a grinder. Five grams of the powder were measured on an electronic balance. The *Syzygium aromaticum* powder was then transferred to a 250 ml conical flask containing 150 ml of distilled water and placed on a rotary shaker at 50°C for 2 hours. The extract was filtered using Whatman No. 1 filter paper. The filtrate can be stored in a refrigerator for up to one week for future use.

Preparation of titanium dioxide solution: -

A 5 mM solution of TiO₂ (MW 79.87 g) was prepared by dissolving it in 100 mL of Sterile distilled water (without any filtration process) and kept on a Magnetic stirrer for two hours.

Synthesis of Syzygium aromaticum titanium dioxide nanoparticles: -

Two Erlenmeyer flasks (250 ml) were labelled as CON. (control) and SATiO₂NP. Eighty mL of a 5 mM solution of TiO_2 was used, excluding the control (100 mL), and incubated for two hours on a magnetic stirrer. Twenty mL of aliquot extract was slowly and carefully added to the flask in a ratio of 4:1 (v: v) under stirring conditions for 4 hours. After four hours, the color of TiO_2 changed due to the plant extracts, while the controls remained unchanged. The formation of nanoparticles was confirmed through the color changes of the reaction mixture. For further processing, the nanoparticles were centrifuged at 5000 rpm for 15 minutes and washed 2-3 times. The pellets were collected and dried in an oven at 45-50°C. The dried powders were prepared for further characterization.

Catalytic activity of Titanium dioxide nanoparticles with dye

The catalytic activity of SATiO₂ NPs was evaluated under dark condition by the reduction of Rhodamine B (RhB), Phenol red (PR), and Bromophenol red (BPR) in the presence of NaBH₄. Aqueous solutions of RhB (0.1 mM), PR (0.1 mM), BPR (0.01 mM), and NaBH₄ (1.0 M) were prepared with sterile distilled water. NaBH₄ was freshly prepared each time before testing. To initiate the catalytic reduction process, a mixture of 2.5 mL of Rhodamine B (0.1 mM) and 0.5 mL of NaBH₄ (0.1 M) was added to the cuvette. A reaction mixture without titanium dioxide nanoparticles served as the control. UV-Visible absorbance spectra were recorded from 200 to 800 nm at 5-minute intervals using a UV-vis spectrophotometer. Then, 1 mg of SATiO₂ NPs was added to each reaction mixture and gently mixed for the interaction of nanoparticles with RhB, PR, and BPR. The decline in dye concentration over time was quantitatively assessed by measuring between 200 and 800 nm with a fixed 20-minute. Following the reaction with nanoparticles, there was a swift reduction in the intensity of the absorption peaks of the dyes at their corresponding wavelengths in the presence of nanoparticles and NaBH₄. The effectiveness of dye degradation was defined using the equation below:

catalytic dye degradation (%) =
$$\frac{(c_0 - c_t)}{c_0} \times 100$$

Where the initial dye concentration is C_0 (without NaBH₄ and nanoparticles), and the concentration of the dye at fixed intervals is C_1 .

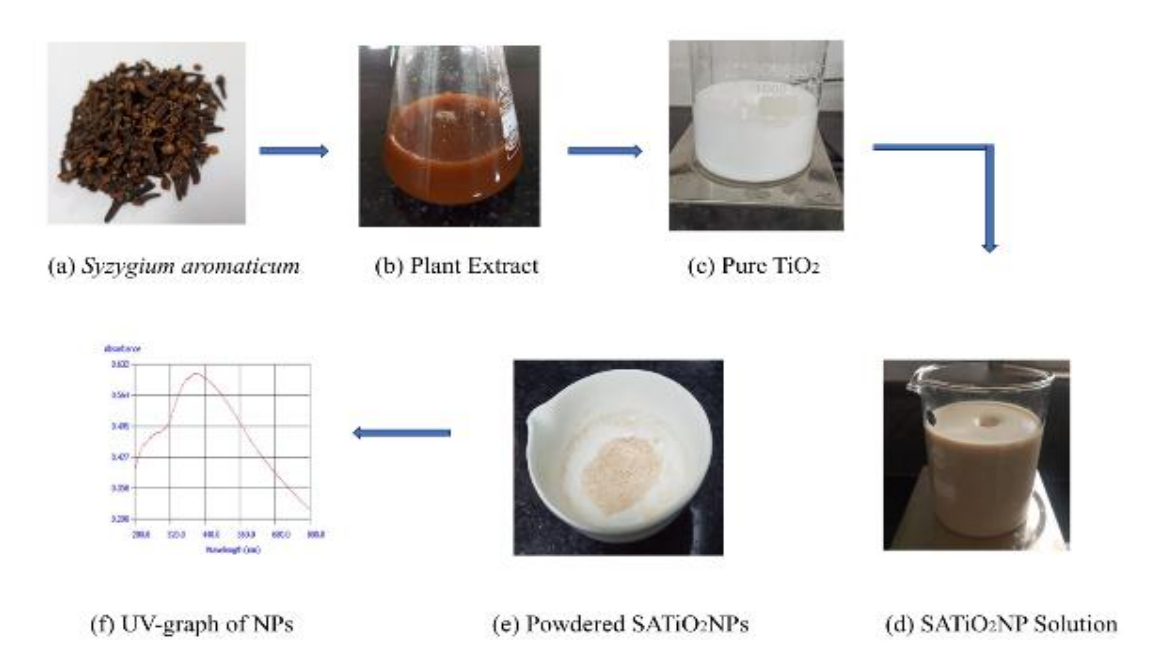


Fig. 1 green synthesis of Szyzgium aromaticum titanium dioxide nanoparticles (flowchart)

CHARACTERIZATION OF SYNTHESIZED NANOPARTICLES

Syzygium aromaticum titanium dioxide nanoparticle (SATiO₂NP) was characterized by a UV-vis spectrophotometer, Fourier Transform Infrared Spectroscopy, Zeta-sizer, and X-ray diffraction.

UV-Visible Spectrophotometer

The formation of nanoparticles and dye degradation were monitored by a UV-visible spectrophotometer (UV-Vis Double Beam Spectrophotometer 2202TS) in the range of 200-800 nm. The energy bandgap of TiO_2NPs was calculated using the equation:

$$Eg = \frac{hc}{\lambda}$$



It depicts the energy bandgap, where h is Planck's constant (4.135 x 10^{-15} eV Hz⁻¹), c is the speed of light (3 x 10^{-8} ms⁻¹), and λ is the wavelength of the radiation (in nm).

Fourier Transform Infrared Spectroscopy (FT-IR Spectroscopy)

FT-IR analysis was used to investigate the functional groups of *Syzygium aromaticum* TiO₂NPs. The FTIR Spectrum-2 (PerkinElmer) was used to examine the FT-IR spectroscopy of green-synthesized *Syzygium aromaticum* titanium dioxide nanoparticles. The sample was stored in an FT-IR sample chamber, and the spectra were collected with 16 scans in the mid-IR range 4000-400 cm-1 for liquid (KBr cell) and solid (in KBr pellets). The interferometer and detection chamber were purged with dry nitrogen to eliminate spectrum interference caused by ambient carbon dioxide and water vapour. Before each sample was analysed, the air background spectrum was recorded.

X-ray Diffraction (XRD)

The purified nanoparticles were obtained by centrifugation at 10000 rpm for 15 minutes, and the pellet was collected. After the lyophilization of the purified nanoparticles, their structure and composition were analysed by XRD and FESEM. The dried mixture of nanoparticles was collected for determining nanoparticle formation using an X-ray diffractometer operated at a voltage of 40 kV and a current of 30 mA with Cu K α radiation in θ -2 θ configurations. The crystallite domain size was calculated from the width of the XRD peaks, assuming they are free from non-uniform strains, using the Scherrer formula.

$$D = \frac{0.94\lambda}{\beta \cos \theta}$$

Where D is the average crystallite domain size perpendicular to the reflecting planes, λ is the X-ray wavelength, β is the full width at half maximum (FWHM), and θ is the diffraction angle.

RESULTS AND DISCUSSIONS

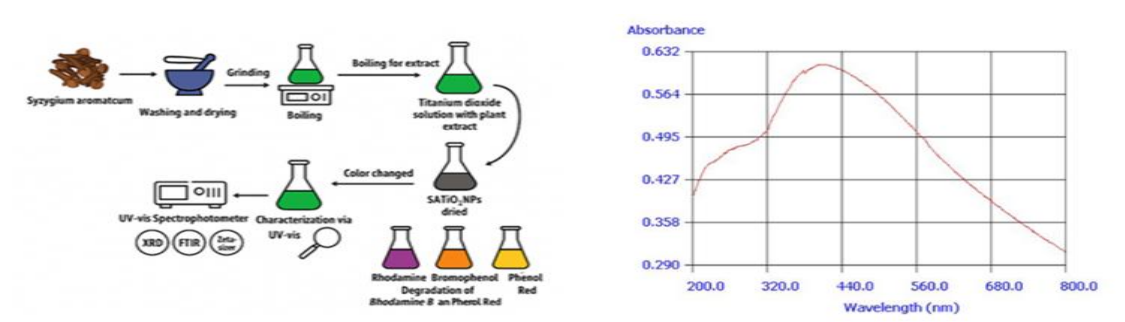


Fig. 2: UV spectra of Titanium dioxide nanoparticles of Syzygium aromaticum (SATiO2NPs)

UV Result:

The creation of SATiO₂NPs was verified by observing changes in the suspension color. The development of TiO₂NPs was monitored regularly using a UV-visible double-beam spectrophotometer across the 200 -800 nm range. The color change occurs due to surface plasmon resonance (SPR) excitation in the TiO₂NPs. It is widely recognized that the optical absorption spectrum of metallic nanomaterials is primarily influenced by surface plasmon resonance. UV-vis absorbance spectroscopy is employed to determine the size of molecules and the band gap of the synthesized titanium dioxide nanoparticles.

The nanoparticles were produced by incorporating plant extracts as a capping agent into a 5 mM TiO₂ solution. The formation of nanoparticles was confirmed by the transition of the white suspension to a coffee color in the case of *Syzygium aromaticum* (SATiO₂NP). The UV-Vis spectral pattern confirmed the presence of colloidal nanoparticles, with the SPR of SATiO₂NPs showing a peak in the absorption spectrum at 378.8nm (Figure 2). The observed color change is again attributed to the excitation of surface plasmon resonance (SPR) in the TiO₂NPs.

FTIR Result

The FTIR spectrum was obtained for the synthesized TiO₂ nanoparticles, utilizing a wave number range of 400-4000 cm-¹ at room temperature, specifically for those created using *Syzygium aromaticum* (SATiO₂NPs). Figure 3 illustrates the FTIR spectra of the synthesized titanium dioxide nanoparticles. This analysis indicated the presence of several functional groups at varying wavelengths. Functional groups such as -CH, -CN, -OH, -CC-, -CO, and -OH may originate from carbohydrates, phenols, tannins, flavonoids, saponins, glycosides, and Steroids found in *Syzygium aromaticum*. These compounds could serve as Capping agents for TiO₂ nanoparticles may also play a significant role in reducing titanium ions to titanium nanoparticles. The characterization of these compounds was performed using FTIR spectra of the catalyst, both with and without the leaf extract addition. Different IR bands were observed at 3715 cm⁻¹, 3387 cm⁻¹, 2184 cm⁻¹, 1707 cm⁻¹, and 683 cm⁻¹ respectively, for TiO₂ NPs. The band at 3715 cm⁻¹ was assigned to the -OH stretching of alcohol, the band at 3387 cm⁻¹ was the characteristic band to N-H stretching of 1° amine, and 2184 cm⁻¹



¹ showed $c \equiv c$ stretching of alkyne. The 1707 cm⁻¹ band indicated the -C-H bending of aromatic compounds. The band at 732 cm⁻¹ and 683 cm⁻¹ was mainly assigned to the Ti-O vibrational mode, confirming the formation of the TiO₂ NPs.

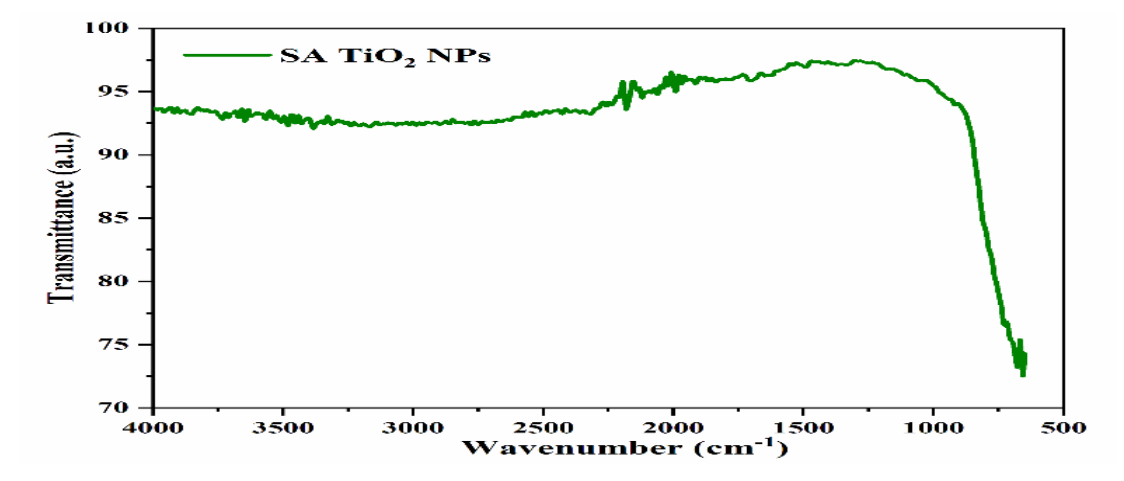


Figure 3: FTIR results of Titanium dioxide nanoparticles of Syzygium aromaticum.

Green samples showed an absorption band in the range 650–700 cm⁻¹, which corresponds to the Ti–O–Ti stretching bond. The absorption peak between the wavenumber range of 650–700 cm-1 is the characteristic peak of the TiO2 NPs anatase phase.

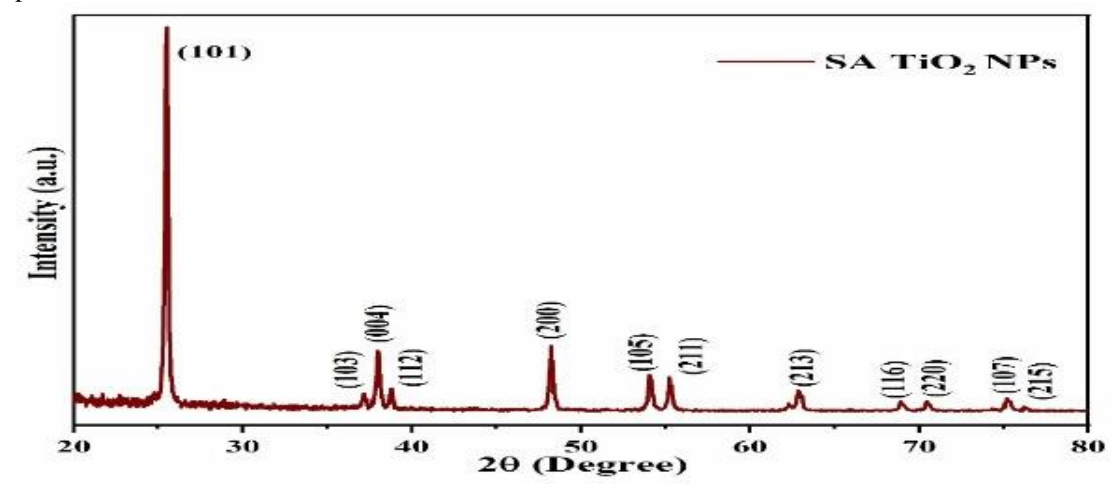


Fig. 4: XRD graph of titanium dioxide nanoparticles of Syzygium aromaticum plant extract.

XRD Result:

Figure 4 shows the X-ray diffraction graph of SATiO₂NPs created from the aqueous extract of *Syzygium aromaticum* buds. The sharp diffraction peaks in the XRD results confirm the high crystallinity of the products. The positions and intensities of these peaks correspond to the tetragonal, anatase polymorph of TiO_2NPs , with the main peak appearing at 25.58° for the (101) plane. Other peak positions include 37.16° (103), 37.98° (004), 38.83° (112), 48.15° (200), 54.15° (105), 55.33° (211), 62.83° (213), 69.00° (116), 70.58° (220), 75.23° (107), and 76.25° (215). A significant peak at 25.58° with high intensity is indicative of the anatase phase of TiO_2NPs at the (101) plane. These values can be well indexed to the anatase structure with a tetragonal crystal form, matching the standard data file (JCPDS no. 75-1537). The products are phase-pure, with calculated lattice constants of a = b = 3.73 Å and c = 9.37 Å. The sharp diffraction peaks in the XRD underline the high crystallinity of the products. The broadening of the peaks is attributed to the nanoscale size of the nanocrystals. The average crystallite size was estimated to be 35.31 nm using Scherrer's formula.

Dye Degradation Results:

In the dye degradation processes, variations in absorbance were observed as the dye broke down over time in the UV spectrum. Initially, Rhodamine B exhibited maximum absorbance at 555 nm and 354 nm, as seen in Figure 5. The peak at 555 nm signified the dye's visible absorption, contributing to its color. Conversely, the peak at 354 nm was associated with a specific electronic transition or absorption characteristic of its molecular structure.



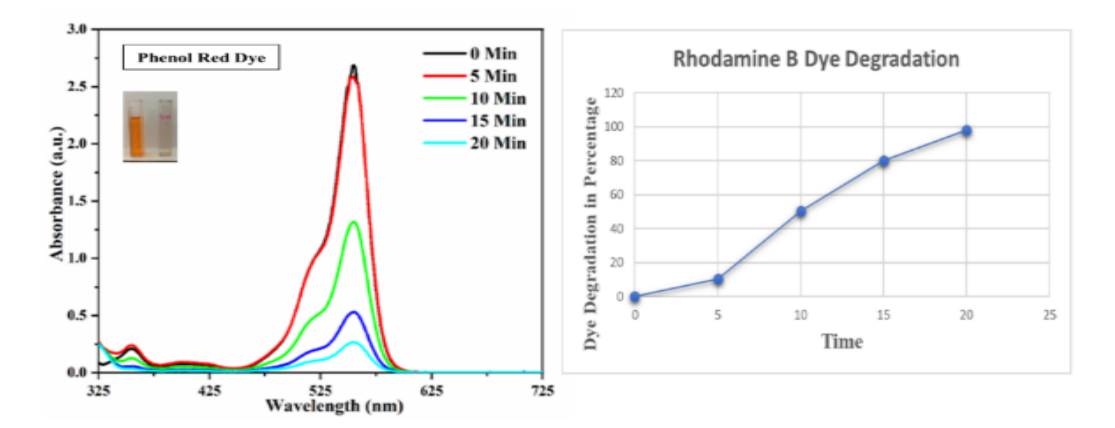


Figure 5: Rhodamine B dye degradation by SATiO₂NPs within 20 minutes.

On the first scan, Rhodamine B was absorbed at 555 nm wavelength. Five minutes later, a second scan was conducted on Rhodamine B degradation in the presence of NaBH₄ and SATiO₂NPs, showing a 10.5 % decrease in absorbance at 554 nm due to initial changes. After 10 minutes, during the third scan, the absorbance at 554 nm decreased by 50.58%, accompanied by a visible loss of color. During the fourth scan, performed at 15 minutes, the absorbance at 554 nm decreased by 80.23%, coinciding with a further decline in color appearance over time. The final scan at 20 minutes demonstrated a decrease in absorbance of 90.5% at 554 nm.

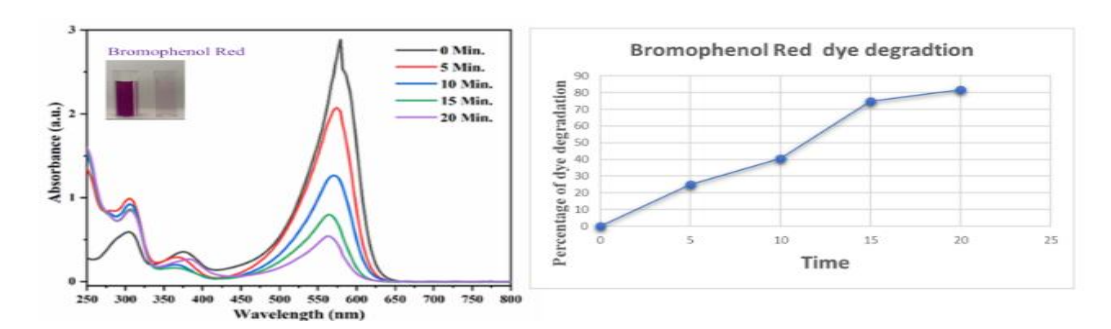


Fig. 6: Bromophenol Red dye degradation by SATiO₂NPs within 20 minutes.

BPR is composed of a phenol ring featuring a bromine and a sulfonate group. The molecular structure of BPR affects its pH-dependent properties, spectroscopic characteristics, and reactivity. The peak at 579 nm is likely associated with the visible absorption of the dye, which varies with pH. This wavelength is generally linked to the dye's red or purple coloration. The peak at 303 nm may relate to the molecular structure or specific functional groups in bromophenol red, such as the aromatic ring or sulfonate group, while the peak at 375.2 nm could be tied to another electronic transition or molecular structure-related absorption.

The initial scan of BPR during the dye degradation showed three primary absorbance peaks at 579 nm, 303 nm, and 375 nm, conducted without $NaBH_4$ and $SATiO_2NP$. The second scan of BPR occurred five minutes post the initial scan with $NaBH_4$ and TiO_2NPs , yielding an absorbance at 574 nm with a 25.10% degradation of the BPR dye. After ten minutes, the third scan recorded an absorbance at 570 nm, reflecting a 40.66% degradation of the BPR dye by nanoparticles. Fifteen minutes later, the fourth scan showed absorbance at 570 nm, with 74.96% degradation of the dye. The fifth scan was completed with an absorbance at 564 nm, marking an 81.68% degradation of the dye. All these scans were performed within 20 minutes and are shown in Figure 6.

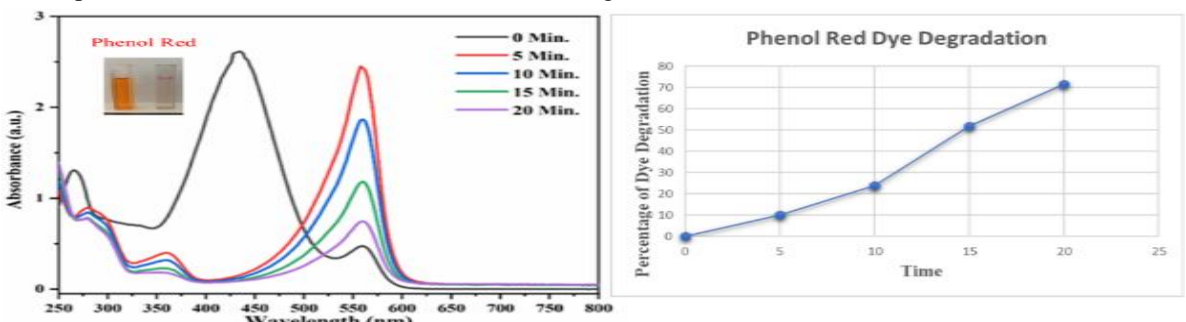


Figure 7: Phenol Red dye degradation by SATiO₂NPs within 20 minutes.



Phenol Red, also known as Phenolsulfonphthalein, is a weak acid used as a pH indicator. Its structure includes a phenolic group and a sulfonphthalein component. It mainly functions as a pH indicator, changing color with pH shifts, and is used in biological research (such as in cell culture media), analytical chemistry (in titrations and assays), and dyeing, primarily as a pH indicator in various solutions rather than as a textile dye.

The UV spectrum of Phenol Red shows absorbance peaks at 435 nm, 560 nm, and 265 nm during initial scans done without nanoparticles and NaBH₄. After adding SATiO₂NPs and NaBH₄ five minutes post initial scan, the absorbance at 435 nm shifted to 557 nm, with a 7.78% decrease in Phenol Red absorbance. A third scan, with Phenol Red, SATiO₂NPs, and NaBH₄ after 10 minutes, showed the same wavelength but a 24% reduction in absorbance at 557 nm, indicating the start of color fading. A fourth scan at 15 minutes revealed a 51.67% decrease, and the final scan at 20 minutes showed a 71.41% reduction in phenol red's absorbance peaks.

CONCLUSION

This study introduces a simple, eco-friendly alternative to traditional physical and chemical methods for producing Titanium dioxide nanoparticles, using aqueous extract of Szyzgium aromaticum as the reducing and stabilizing agent. The biosynthesis process was optimized based on the SPR absorption bands of metallic nanoparticles. Characterized by UV-vis, FTIR, and XRD, the nanoparticles showed high crystallinity with an average size of 329.5 nm. The crystallite size was estimated at 35.31 nm using Scherrer's formula. The catalytic properties of these nanoparticles were tested for degrading Bromophenol red, Phenol red, and Rhodamine B in the presence of sodium borohydride in water. This study highlights the potential of biosynthesized titanium dioxide nanoparticles as environmentally friendly catalysts for removing pollutants from industrial effluents.

Conflict of Interest: The authors declare no competing interests in this work.

Funding: No (Any funding)

REFERENCES

- 1. Singh, D., Tiwari, A., Singh, R. P., and Singh, A. K. (2024). Clove bud extract mediated green synthesis of bimetallic Ag–Fe nanoparticles: antimicrobial, antioxidant and dye adsorption behaviour and mechanistic insights of metal ion reduction. *Mat. Chem. Phys.* 311, 128529. doi: 10.1016/j.matchemphys.2023.128529
- 2. Hameed, M., Rasul, A., Waqas, M. K., Saadullah, M., Aslam, N., Abbas, G., et al. (2021). Formulation and evaluation of a clove oil-encapsulated nanofiber formulation for effective wound-healing. *Molecules* 26, 2491. doi:10.3390/molecules26092491
- 3. Ricardo-Rodrigues, S., Rouxinol, M. I., Agulheiro-Santos, A. C., Potes, M. E., Laranjo, M., and Elias, M. (2024). The antioxidant and antibacterial potential of thyme and clove essential oils for meat preservation—an overview. *Appl. Biosci.* 3, 87–101. doi:10.3390/applbiosci3010006
- 4. Maggini, V., Semenzato, G., Gallo, E., Nunziata, A., Fani, R., & Firenzuoli, F. (2023). Antimicrobial Activity of *Syzygium aromaticum* Essential Oil in Human Health Treatment. *Molecules*, 29(5), 999. https://doi.org/10.3390/molecules29050999
- 5. Lakhan, M. N., Chen, R., Shar, A. H., Chand, K., Shah, A. H., Ahmed, M., et al. (2020). Eco-friendly green synthesis of clove buds extracts functionalized silver nanoparticles and evaluation of antibacterial and anti-diatom activity. *J. Microbiol. Met.* 173, 105934.doi: 10.1016/j.mimet.2020.105934
- 6. Xu, Y., Chen, H., Zhang, L., and Xu, Y. (2023). Clove essential oil loaded chitosan nanocapsules on quality and shelf-life of blueberries. *Int. J. Biol. Macromol.* 249, 126091. doi: 10.1016/j.ijbiomac.2023.126091
- 7. Edis, Z., Haj Bloukh, S., Ashames, A. A., M., M., Shahwan, M. J., Abu Sara, H., Boddu, S. H., Khan, S. N., Bloukh, I. H., Eladdasy, M., Sadeghi, S., Alkubaisi, H., Bloukh, I. H., & Hassan, N. A. (2025). Syzygium aromaticum extract mediated, sustainable silver nanoparticle synergetic with heterocyclic antibiotic clarithromycin, and their antimicrobial activities. *Frontiers in Chemistry*, *12*, 1513150. https://doi.org/10.3389/fchem.2024.1513150
- 8. Irshad, M.A., Nawaz, R., Rehman, M.Z., Imran, M., Ahmad, M.J., Ahmad, S., Ali, S., 2020. Synthesis and characterization of titanium dioxide nanoparticles by chemical and green methods and their antifungal activities against wheat rust. *Chemosphere* 258, 127352.
- 9. Sethy, N.K., Arif, Z., Mishra, P.K., Kumar, P., 2020. Green synthesis of TiO2 nanoparticles from *Syzygium cumini* extract for photo-catalytic removal of lead (Pb) in explosive industrial wastewater. *Green Process. Synth.* 9 (1), 171–181
- 10. Goutam, S.P., Saxena, G., Singh, V., Yadav, A.K., Bharagava, R.N., Thapa, K.B., 2018. Green synthesis of TiO₂ nanoparticles using leaf extract of *Jatropha curcas L*. for photocatalytic degradation of tannery wastewater. *Chem. Eng.* J. 336, 386–396.
- 11. Krishnasamy, A.; Sundaresan, M.; and Velan, P. (2024), Rapid photosynthesis of nano-sized titanium using leaf extract of *Azadirachta indica*. *International Journal of Chemtech Research*, Vol 8, No.4, pp 2047-2052,



- Artificial Cells, Nanomedicine, and Biotechnology, Vol. 52, NO. 1, 1–11, https://doi.org/10.1080/21691401.2023.2301068
- 12. Girigoswamia, A., Deepika, B., Panduranganb, A.K., and Girigoswamia, K., 2024, Preparation of titanium dioxide nanoparticles from *Solanum Tuberosum* peel extract and its applications. *Artificial Cells, Nanomedicine, and Biotechnology*, (2024), VOL. 52, NO. 1, 1–11, https://doi.org/10.1080/21691401.2023.2301068
- 13. Raliya, R., Biswas, P., & Tarafdar, J. (2015). TiO2 nanoparticle biosynthesis and its physiological effect on mung bean (Vigna radiata L.). *Biotechnology Reports*, *5*, 22-26. https://doi.org/10.1016/j.btre.2014.10.009
- 14. Aswini, R.; Murugesan, S.; & Kannan, K. Bio-engineered TiO2 nanoparticles using *Ledebouria revoluta* extract: Larvicidal, histopathological, antibacterial and anticancer activity. *International Journal of Environmental Analytical Chemistry* 2021, 101, 2926-2936, https://doi.org/10.1080/03067319.2020.1718668
- 15. Rajkumari, J., Magdalane, C. M., Siddhardha, B., Madhavan, J., Ramalingam, G., Al-Dhabi, N. A., Arasu, M. V., Ghilan, A., Duraipandiayan, V., & Kaviyarasu, K. (2019). Synthesis of titanium oxide nanoparticles using Aloe barbadensis mill and evaluation of its antibiofilm potential against Pseudomonas aeruginosa PAO1.

 Journal of Photochemistry and Photobiology B: Biology, 201, 111667.

 https://doi.org/10.1016/j.jphotobiol.2019.111667
- 16. Hossain, A., Abdallah, Y., Ali, M. A., Masum, M. M., Li, B., Sun, G., Meng, Y., Wang, Y., & An, Q. (2019). Lemon-Fruit-Based Green Synthesis of Zinc Oxide Nanoparticles and Titanium Dioxide Nanoparticles against Soft Rot Bacterial Pathogen Dickeya dadantii. *Biomolecules*, 9(12), 863. https://doi.org/10.3390/biom9120863
- 17. Subhapriya, S., & Gomathipriya, P. (2018). Green synthesis of titanium dioxide (TiO2) nanoparticles by Trigonella foenum-graecum extract and its antimicrobial properties. *Microbial Pathogenesis*, *116*, 215-220. https://doi.org/10.1016/j.micpath.2018.01.027
- 18. Saranya, K. S., Senan, C., Pilankatta, R., Saranya, K., George, B., Wacławek, S., & Černík, M. (2018). Green Synthesis of High Temperature Stable Anatase Titanium Dioxide Nanoparticles Using Gum Kondagogu: Characterization and Solar Driven Photocatalytic Degradation of Organic Dye. *Nanomaterials*, 8(12), 1002. https://doi.org/10.3390/nano8121002
- 19. Zhang, Y., Zhang, C., Liu, K., Zhu, X., Liu, F., & Ge, X. (2018). Biologically synthesized titanium oxide nanostructures combined with morphogenetic protein as wound healing agent in the femoral fracture after surgery. *Journal of Photochemistry and Photobiology B: Biology*, 182, 35-41. https://doi.org/10.1016/j.jphotobiol.2018.03.005